J Appl Electrochem (2007) 37:1515–1522
DOI 10.1007/s10800-007-9423-0

ORIGINAL PAPER

Reductive annealing for generating Se doped 20 wt% Ru/C cathode catalysts for the oxygen reduction reaction

K. S. Nagabhushana · E. Dinjus · H. Bönnemann · V. Zaikovskii · C. Hartnig · G. Zehl · I. Dorbandt · S. Fiechter · P. Bogdanoff

Received: 10 November 2006 / Revised: 10 September 2007 / Accepted: 12 September 2007 / Published online: 12 October 2007

Abstract Reductive annealing was chosen as a method for the syntheses of Se modified Ru/C catalysts. Initial preparation of a 20 wt% Ru/C was performed by impregnating $RuCl_3 \cdot 2H_2O$ on Vulcan XC72 with subsequent conditioning using H_2 at 250 °C for 4 h. Surface treatment of Ru/C by SeO_2 followed by reductive annealing produced Se modified Ru/C catalysts with a pre-determined Ru:Se = 1:0.15 and 1:1 a/o. Structural characterization was carried out using HRTEM while electrochemical characterization was performed using RDE measurements. It is concluded that the presence of Se on Ru has a positive effect on the oxygen reduction reaction of RuSe/C catalyst systems with an optimal loading of Se close to a Ru:Se ratio of 1:0.15 a/o. Overloading of selenium led to neutralization of its promoting effect.

Keywords Oxygen reduction reaction · RuSe electrocatalysts · Core-shell structure · Reductive annealing · Cathode catalyst

K. S. Nagabhushana · E. Dinjus · H. Bönnemann
Forschungszentrum Karlsruhe, ITC-CPV, Postfach 3640, 76021 Karlsruhe, Germany

K. S. Nagabhushana · E. Dinjus
Ruprecht-Karls-Universität Heidelberg, Seminarstrasse 2, 69117 Heidelberg, Germany

Present Address:
K. S. Nagabhushana (✉)
Department of Chemistry, MIT, Manipal 576104, India
e-mail: ks.nagabhushana@manipal.edu

H. Bönnemann
Max-Planck Institüt für Kohlenforschung, 45470 Mulheim an der Ruhr, Germany

V. Zaikovskii
Boreskov Institute of Catalysis, Russian Academy of Sciences, Pr. Akademika Lavrentieva 5, 630090 Novosibirsk, Russia

C. Hartnig
Centre for Solar Energy and Hydrogen Research (ZSW), ECW/ECV, Helmholtzstr. 8, 89081 Ulm, Germany

G. Zehl · I. Dorbandt · S. Fiechter · P. Bogdanoff (✉)
Hahn-Meitner-Institute Berlin GmbH, Solare Energetik SE-5, Glienicker Strasse 100, 14109 Berlin, Germany
e-mail: bogdanoff@hmi.de

1 Introduction

Synthesis of active fuel cell catalysts for the cathode side of a low temperature Fuel Cell is a demanding task since even the best of catalysts tested suffer from significant overpotential for the oxygen reduction to a magnitude of 0.3 V [1]. In addition, formation of corrosive hydrogen peroxide under operating conditions can severely damage crucial cell components including catalysts, gas diffusion layers and proton conducting membranes. Therefore, oxygen reduction reaction (ORR) catalysts with repressed selectivity towards H_2O_2, are highly recommended.

For activity, stability and economic reasons, Pt with other metals like Fe [2], Co [2–4], Ni [2–5], and Cr [6] were studied as new cathode catalyst systems. In addition, platinum free, Ru chalcogenides (Ru_xSe_y) have been extensively studied as methanol tolerant ORR catalysts [7–11]. Recently, colloidal synthesis was performed [12] to generate catalysts by surface doping Ru/C with increasing amounts of Se with $0 \leq Se/Ru \leq 1$. Physical characterization revealed the formation of a core-shell structure, especially for the higher loadings of Se on Ru, with Ru nanoparticles showing limited agglomeration during the Se doping step. Further, for higher Se loadings, formation of a

Se containing shell was seen uniformly around the Ru core, indicating a stable ruthenium selenide compound formed by the extraction of surface Ru atoms in the core. While the formation of Ru_xSe_y was confirmed by physical characterization, a mechanism which explains the basis of such a drastic positive effect of Se on Ru/C catalyst is not yet well understood.

Subtle changes in the synthesis are known to play a pivotal role on the structure of RuSe nanoparticles implying change in their electrochemical properties [12–15]. Hilgendorff et al., showed that RuSe catalyst prepared via thermolysis of Ru-carbonyl led to distinct aggregation and moderate activity [14]. To overcome this problem, colloidal techniques were applied to obtain better particle distribution and higher activity [12]. However, this technique is too complex for the preparation of higher amounts of active catalyst, as required for technical applications. Here we report a simple reductive annealing procedure for the synthesis of Ru_xSe_y/C catalysts with Ru_1Se_0, $Ru_1Se_{0.15}$ and Ru_1Se_1 for the ORR as part of a concerted and continued effort to find an active and optimum Se modified Ru/C catalyst.

2 Experimental

2.1 Synthesis of the catalyst

The synthesis was performed in two steps. As a primary source, and a control for comparing the electrochemical properties, 20 wt% of Ru/C catalyst was generated and Se was doped at the surface of Ru, in different amounts, to generate 1:1 a/o and 1:0.15 a/o Ru:Se/C catalysts.

2.2 Preparation of 20 wt% Ru/C (Vulcan XC72) catalyst

In a 1 L two neck round bottom flask, 2.43 g of $RuCl_3{\cdot}2H_2O$ (10 mmol) was suspended in 500 mL of THF and 25 mL of argon saturated UHQ water was added to completely dissolve the salt. After stirring at room temperature for 30 min., 4.0 g of Vulcan XC72 was introduced and the whole mixture was stirred for a further 4 h at room temperature. The solvent was then evaporated under reduced pressure (5×10^{-2} mbar) and the resulting free flowing solid was reductively annealed using a conditioning apparatus [16] under hydrogen (5.0 purity, 10 NL h^{-1}) flow at 250 °C for 4 h and the sample tube was cooled while purging with argon. The conditioned material suspended in water did not yield a colored solution indicating complete reduction of $RuCl_3$ to metallic ruthenium.

2.3 Preparation of Se doped 20 wt% Ru/C catalysts

In a 100 mL volumetric flask, 1.0 g of SeO_2 dissolved in THF:H_2O (80:20 v/v) was prepared. In order to generate 1:1 a/o of Se:Ru/C catalyst, 2.0 g of 20 wt% Ru/C was suspended in 200 mL of THF and to this 44 mL of SeO_2 solution was added. The whole suspension was stirred at room temperature for 2 h and the solvent evaporated under reduced pressure. The material was conditioned using hydrogen at 250 °C for 2 h to generate Ru(17.3 wt%)Se(13.5 wt%)/C catalyst with Ru:Se = 1:1 (a/o). Similarly, using 3.29 mL of SeO_2 solution added to 1.5 g of 20 wt% Ru/C catalyst, a 1:0.146 a/o of Ru (19.6 wt%)Se(2.2 wt%)/C catalyst was generated.

For simplicity of identifying these two Se doped catalysts a 1:1 a/o catalyst is reported as Ru_1Se_1/C catalyst while the one with 1:0.146 a/o is reported as $Ru_1Se_{0.15}$/C catalyst.

2.4 Structural characterization

HRTEM images were obtained on a JEM-2010 electron microscope (JEOL, Japan) with a lattice-fringe resolution of 0.14 nm at an accelerating voltage of 200 kV. The high-resolution images of periodic structures were analyzed by the Fourier method. Local energy-dispersive X-ray analysis (EDX) was carried out on an EDAX spectrometer (EDAX Co.) fitted with a Si (Li) detector with a resolution of 130 eV. Samples to be examined by HRTEM were prepared on a perforated carbon film mounted on a copper grid.

2.5 Electrochemical measurements

Cyclic voltammetry and rotating-disc electrode (RDE) measurements were performed in a conventional three-compartment electrochemical glass cell, in which a mercury sulphate electrode was used as the reference (650 mV vs. NHE) and a platinum wire as counter electrode. The catalyst powder was attached to the working electrode, which was a Teflon surrounded glassy carbon (GC) rod (3 mm in diameter). The catalyst powder (1 mg) was ultrasonically suspended in 200 μL of a 0.2 wt% Nafion-solution (Aldrich). A 5 μL of this suspension was transferred onto the glassy carbon disc of the electrode and dried in air at 60 °C. The measurements were performed at room temperature in 0.5 M H_2SO_4 saturated with oxygen and nitrogen for the RDE measurement and the cyclic voltammetry, respectively.

3 Results and discussion

The synthesis of the catalysts is schematically depicted in Fig. 1. The synthesis was performed using reductive annealing as a method, since preparation of Ru by the colloidal route produced agglomeration during the Se addition step, though well dispersed, uniformly distributed Ru metal particles were seen after the initial synthesis step. Reduction of $RuCl_3$ to metallic ruthenium in the presence of hydrogen is known to occur at temperatures in the region of 300 °C [17]. Preparation of Ru nanoparticles on titania support in the size domain 1.5 ± 0.25 nm was achieved with a metal loading of 1.5 wt%. However, in the present study, with an increased loading of Ru (20 wt%) on the support surface with reductive annealing at 250 °C, sintering of the Ru metal nanoparticles is expected. Having no stabilizers to control the size of the nanoparticles, except for the heterogeneous carbon support, a non-uniform size distribution of metal nanoparticles is expected. Figure 2 provides the Transmission Electron Micrographs (TEMs) of the parent 20 wt% Ru/C (Vulcan XC72) catalyst that served as the starting material for Se doped catalysts. From the micrographs 2A and B, dispersed and aggregated Ru nanocrystals (size ranging from 1 to 10 nm) on the carbon surface are present, reflecting the method of preparation. The metal nanoparticle-support interaction is at least in part due to the characteristics of the Carbon support and a forthcoming article highlights these aspects. Figure 2C provides the HRTEM image of Ru aggregates and an increased magnification provided in Fig. 2D shows periodic fringes, corresponding to lattice planes of Ru crystal: d_{100} = 0.234 nm, d_{002} = 0.215 nm, d_{101} = 0.205 nm. Some structural disordering (arrow marked) observed on the surface of the Ru particles may be accounted for by surface oxidation of Ru under ambient conditions.

Addition of SeO_2 using a mixture of 8:2 v/v of THF and H_2O is carried out to minimize the dissociation of selenious acid and prevent agglomeration of the Ru nanoparticles by etching during the modification step. Formation of a uniform layer of SeO_2 on Ru nanoparticles, which subsequently undergo reaction with the surface Ru atoms during reductive annealing, yields a stable compound as a shell around the Ru nanoparticle. As described later, low Se content enhances the activity of ORR by one order of magnitude compared to Se free Ru/C catalyst. Therefore, with increased Se loadings one should expect further growth of the catalytically active surface layer resulting in enhancement of catalytic activity. However, the electrochemical results clearly show a strong decrease in the catalyst activity at high amounts of selenium. In order to clarify this unexpected behavior at high selenium loadings, HRTEM investigations were performed.

Figure 3 shows the Ru_1Se_1/C catalyst with 3A providing a lamellar core-shell structure of aggregated composite Ru–Se nanoparticles having 1 or 2 lamellar layers (shells) of ruthenium selenide formed on the surface of relatively big Ru particles (core). Figure 3B provides the HRTEM periodic image of fringes from Ru and ruthenium selenide lattice (insert from A). In the bi-layered RuSe shell containing nanoparticles, the spacing between two lamellar layers of ruthenium selenide is 0.6–0.7 nm with a periodicity of 0.24–0.27 nm for the ruthenium selenide unit in the layer (Fig. 3B). A similar structure was observed for identical loadings of Se on Ru nanoparticles prepared via the colloidal route [12]. Formation of hollow-core spherical structures (Kirkindall effect) of smaller ruthenium selenide composites is also evidenced (Fig. 3C, D) [12]. From the EDX analysis (Table 1), nominal Ru:Se ratios were seen, indicating that most of the Se is located on the Ru nanoparticles which corroborates the findings from HRTEM (Fig. 3). In essence, surface doping of Se on Ru has been effectively achieved with most of the added Se residing on the core Ru nanoparticle and in the 1:1 a/o, a uniform lamellar structure being formed on the surface of the Ru nanoparticles. However, the following electrochemical results reveal that this well identified structure is not responsible for the high catalytic activity found at moderate selenium contents. TEM images of the $Ru_1Se_{0.15}/C$

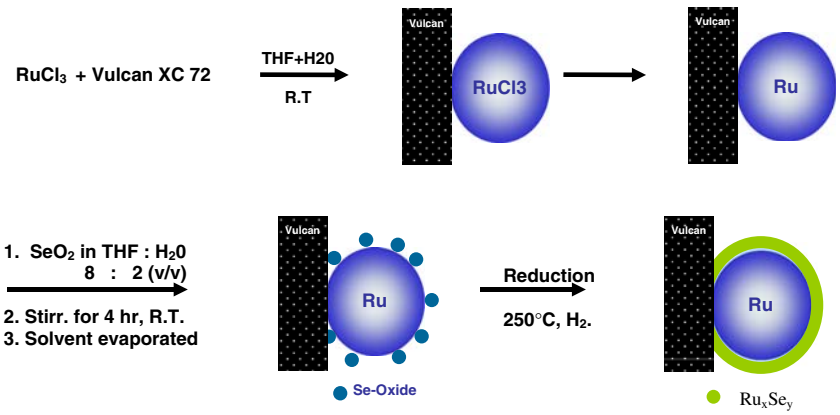

Fig. 1 Schematic representation of the synthesis of Se doped Ru/C catalysts

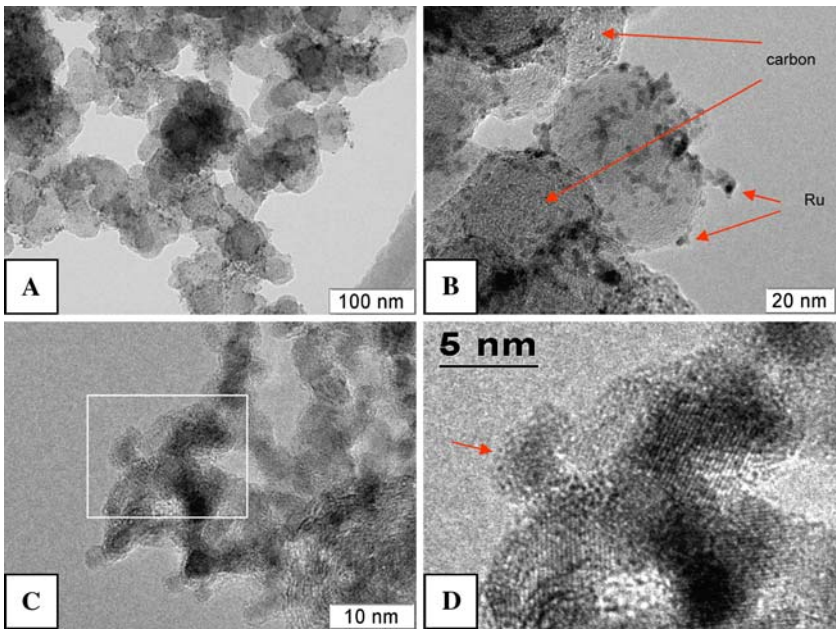

Fig. 2 TEM micrographs of 20% Ru on Vulcan XC72; (**A**) and (**B**) provides the distribution of Ru nanocrystals on the Carbon surface while (**C**) and (**D**) shows HRTEM of the Ru aggregates. Scale bars are provided for clarity

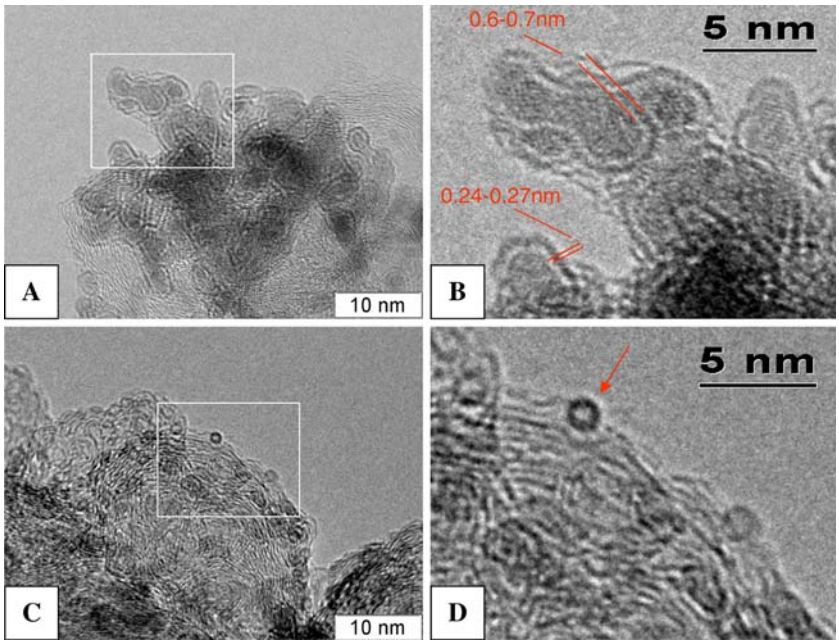

Fig. 3 HRTEM of Ru_1Se_1/C catalyst; Sub divisions (**A**) indicate a lamellar core-shell structure of RuSe composites. (**B**) HRTEM periodic image of fringes from Ru and ruthenium selenide lattice. (**C**) spherical RuSe composite structures without Ru core. (**D**) Increased insert from "C" of smallest Ru–Se composites ($\sim$1 nm, arrowed). Scale bars are provided for clarity

(Vulcan XC72) catalyst are presented in Fig. 4. Micrographs 4A and B show particle distributions similar to the images taken from the Se free Ru/C catalysts, presented in Fig. 2. The distributions of $RuSe_x$ nanoparticles appear non-uniform over the Vulcan XC72 carbon beads. Therefore, the higher catalytic activity of this material compared to the Ru/C- and Ru_1Se_1/C-samples cannot be explained by better dispersion of the catalytically active compound. Highly resolved images of the $Ru_1Se_{0.15}$/C catalyst are depicted in Fig. 4C and D. The size of the distinct $RuSe_x$ nanocrystallites ranges from 2 to 5 nm. However, in contrast to the Ru_1Se_1/C catalyst (see Fig. 3), these particles do not exhibit any visible lamellar shells around compact cores. Nevertheless, effective selenium doping of Ru crystallites during catalyst preparation took place. EDX analysis on $Ru_1Se_{0.15}$/C catalyst sample revealed no detectable Se concentration directly on Vulcan XC72, indicating that most of the Se interacts strongly with Ru particles. However, for the most active $Ru_1Se_{0.15}$/C catalyst, no ruthenium selenide coverage on the particles was

Table 1 Ru:Se ratio of the Ru(20%)/C and of the selenium doped $Ru_1Se_{0.15}$/C and Ru_1Se_1/C catalysts, measured by EDXA from metal and composite particles, respectively

	Se L_α:Ru L_α
Ru(20%)/C	0:100
$Ru_1Se_{0.15}$/C	6:94
Ru_1Se_1/C	48:52

The signal ratios of the Si L_α- and Ru L_α-lines were evaluated

detected. Therefore a different surface structure at low selenium contents is likely. Further work is expected to confirm this.

3.1 Cyclic voltammetry

The catalysts were electrochemically characterized by cyclic voltammetry in 0.5 M H_2SO_4 purged with nitrogen in a GC/RDE assembly. All samples were cycled between 0 and 0.85 V vs. NHE at a scan rate of 50 mV s^{-1}. The voltammograms are shown in Fig. 5a–c, where Fig. 5a depicts the voltammogram of the selenium free Ru(20 wt%)/Vulcan catalyst and Fig. 5b, c represent the ruthenium catalyst modified with $Ru_1Se_{0.15}$/C and Ru_1Se_1/C, respectively. With the unmodified catalyst (Fig. 5a) in the range 0.1–0.3 V, a peak appears in the negative scan which is accounted for by the reduction of a ruthenium surface oxide film. In the region 0.2–0.7 V an increasing anodic current was observed caused by overlapping of two stages of the ruthenium surface oxidation (Ru(0) to Ru(I) and Ru(II)) as suggested by Conway et al. [18]. A similar result was obtained for the $Ru_1Se_{0.15}$/C catalyst, although the peaks are broadened and the oxide reduction peak is shifted by approximately 100 mV towards higher potential. This indicates higher catalyst reducibility, probably caused by changes in the oxide coverage of the electrode (Fig. 5b). Whether this is due to the formation of mixed oxygen–selenium coverage of the ruthenium particles or to a catalytic influence of selenium on the ruthenium reducibility cannot be concluded from these measurements. However, a distinct modification of the ruthenium surface took place, leading to a 10-fold increase in the kinetic current density (Table 2) as deduced from the RDE measurements. For the Ru_1Se_1/C catalyst, the capacitive current is significantly decreased and no significant red-ox peaks were seen (Fig. 5c). This corroborates with the observed substantial reduction in the oxidation of ruthenium nano-particles modified with higher amounts of selenium [19, 20], which coincides with the HRTEM results, revealing a complete transformation of the Ru-surface into a crystalline Ru_xSe_y compound. The kinetic current density of this catalyst was found to be nearly the same as for the sample without selenium modification (Table 2). This finding supports results obtained for Se modified unsupported Ru catalysts prepared by thermolysis of $Ru_3(CO)_{12}$, where the catalytic activity for oxygen reduction was found to decrease again above a selenium content of 15 mol% [21]. Thus, the current result once more points towards the existence of an optimum amount of selenium to modify the surface of the ruthenium nanoparticles. Investigations towards the optimization of the Ru:Se ratio, already reported [19].

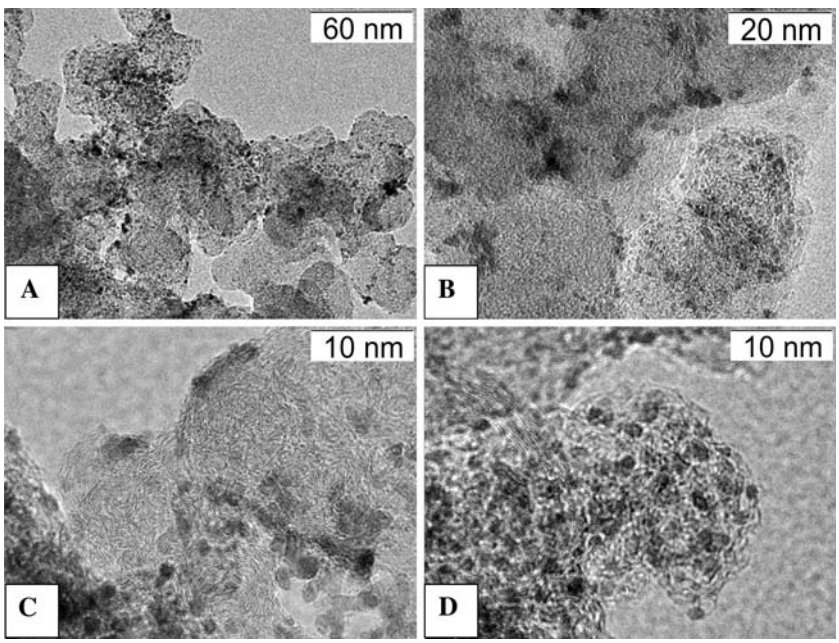

Fig. 4 TEM of the $Ru_1Se_{0.15}$/C catalyst; Sub divisions (**A**) and (**B**) show the distribution of $RuSe_X$ nanoparticles on the carbon support while (**C**) and (**D**) provide higher resolved images of discrete particles in a size domain of 2 nm. Scale bars are given top right within every sub division

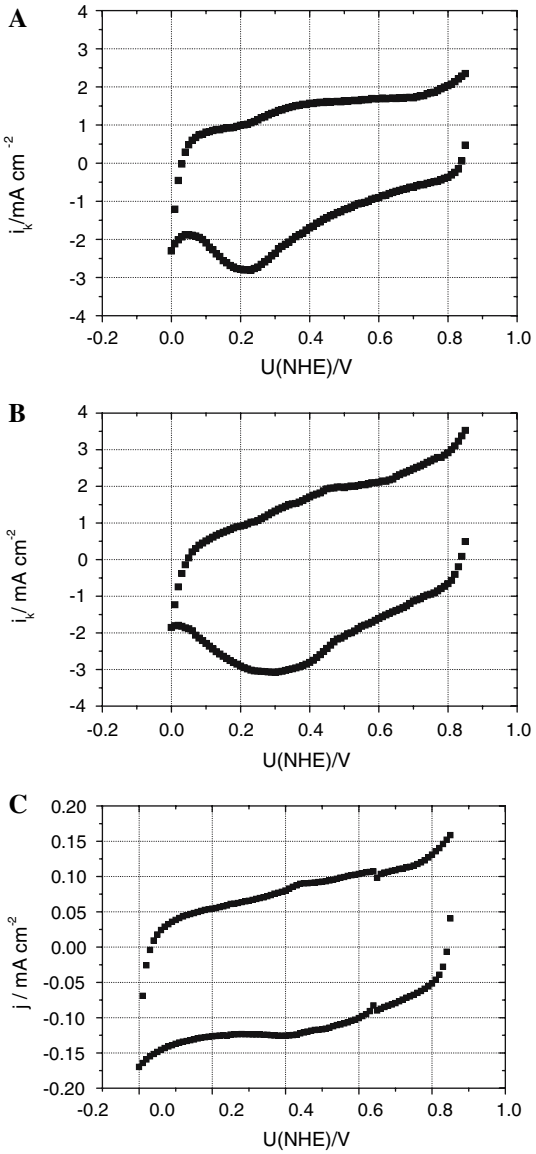

Fig. 5 Cyclic voltammograms of the selenium free Ru (20 wt%)/C catalyst (**A**) and of the selenium modified catalysts $Ru_1Se_{0.15}$/C (**B**) and Ru_1Se_1/C (**C**)

3.2 Oxygen reduction in RDE measurements

It is known that the measured current j at a disc electrode covered with a catalyst film for first order reaction kinetics is given by:

$$\frac{1}{j} = \frac{1}{j_k} + \frac{1}{j_D} = \frac{1}{j_k} + \frac{1}{B\omega^{1/2}} \tag{1}$$

where j_k is the kinetic contribution to the current in the absence of mass transfer effects, j_D is the limiting diffusion current density, ω is the rotation rate of the electrode and B the Levich constant given by the equation:

Table 2 Tafel slopes for the Ru(20%)/C (a), the $Ru_1Se_{0.15}$/C (b) and the Ru_1Se_1/C (c) catalyst

	j_k (mA cm^{-2})	b (mV dec^{-1})
Ru(20%)/C	0.19	112.5
$Ru_1Se_{0.15}$/C	1.91	102.8
Ru_1Se_1/C	0.12	109.7

$$B = 0.62 n_e F D^{2/3} c_{o_2} v^{-1/6} \tag{2}$$

where n_e is the number of electrons transferred per O_2 molecule, F the Faraday constant, D the diffusion coefficient, c_{o_2} the O_2 concentration in solution, and v the kinematic viscosity of the electrolyte.

The Tafel slope (Fig. 6) was obtained from the mass transfer corrected plot of E versus $\log[j_D/(j_D - j)]$. Each line represents the average curve obtained from two measurements at five different RDE rotation rates ranging from 200 to 2,500 rpm. In Table 2 the Tafel slopes are summarized. In all experiments, we compared the corrected j_k of the Tafel plot at a potential of 0.7 V vs. NHE.

Although a significant change in the kinetic current densities was observed from the 20 wt% Ru/C catalyst without selenium towards a selenium content of 1.6 wt% (molar ratio Ru:Se = 1:0.15) the Tafel slopes showed no significant change. As depicted by the current densities in Table 2, modification of the ruthenium surface with selenium leads to a significant increase in the catalytic activity. Addition of excess selenium nullifies the observed promoting effect as observed for the $Ru_1Se_{0.15}$/C catalyst. The results strongly suggest the formation of an inactive crystalline Ru_xSe_y compound on the ruthenium surface when the Se content is high, having a different structure to that of the low selenium loaded, highly active catalyst.

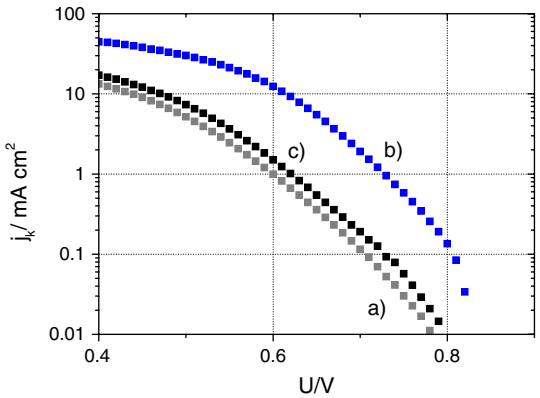

Fig. 6 Tafel plots for the Ru(20%)/C (**a**), the $Ru_1Se_{0.15}$/C (**b**) and the Ru_1Se_1/C (**c**) catalyst

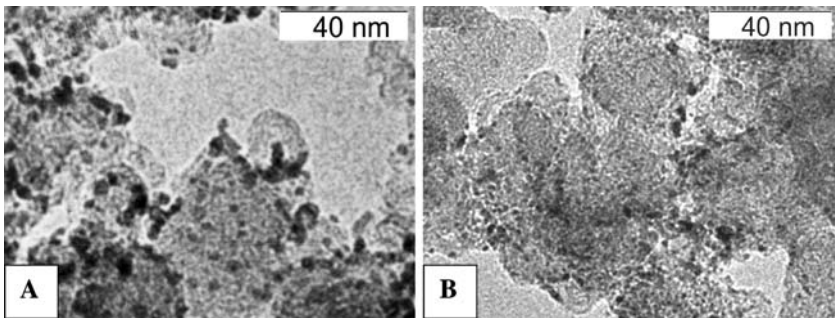

Fig. 7 TEM of the $Ru_1Se_{0.15}$/C catalysts: A depicts a sample from colloidal preparation method [12] while B shows a similar catalyst prepared by impregnation technique within this work at the same enlargement (for higher resolved images see Fig. 4). Scale bars are given top right within every sub division

3.3 Catalyst preparation by reductive annealing versus colloidal preparation technique

The colloidal preparation route towards carbon supported RuSe electrocatalysts produced highly active materials. This higher catalytic activity, compared to catalysts prepared via thermolysis of $Ru_3(CO)_{12}$ in Se saturated xylene [11] was attributed to the superior dispersion of the active compounds [12]. However, the colloidal route demands stringent conditions and are a serious hindrance to any industrial scale-up. Therefore, an important motivation for the present work was to simplify the preparation technique while maintaining the advantageous ORR activity.

In a model study, $Ru_1Se_{0.15}$/C catalyst was prepared by the colloidal method and physical and electrochemical characterizations were performed [12]. In brief, anhydrous $RuCl_3$ and Vulcan XC72 were suspended in dry THF under inert atmosphere. $LiBet_3H$ served as reducing agent to generate colloidal metal nanoparticles which were uniformly loaded on to Vulcan XC72. Highly dispersed Ru/C powder generated in this way was modified with Se using SeO_2 dissolved in THF and water. The limiting current density for this catalyst derived from RDE measurement was 2.07 mA cm^{-2}, which is close to the value of 1.91 mA cm^{-2} derived for the $Ru_1Se_{0.15}$/C impregnation catalyst prepared within this work (see Table 2). The particle size distributions of both catalysts were assessed by TEM, as shown in Fig. 7. The $Ru_1Se_{0.15}$/C colloidal catalyst (Fig. 7A) features generally larger crystallite sizes of the Se doped ruthenium particles, but a more uniform distribution over the carbon support, compared to the $Ru_1Se_{0.15}$/C impregnation catalyst (Fig. 7B). However, this difference has not caused significant change in the catalytic activity owing to the absence of distinct particle aggregation on both catalyst types at ruthenium loadings of 20 wt%. At higher Ru content, this difference can be significant with the colloidal techniques providing better catalyst with better dispersion of the metal nanoparticles. This will be the subject of further investigation.

4 Conclusion

Preparation of $RuSe_x$/C electrocatalysts using the reductive annealing technique represents an easier preparation route in comparison to colloidal synthesis. At a ruthenium content of 20 wt%, the catalysts obtained via both preparation routes have comparable catalytic activity. Since a chemical compound is formed at the surface of Ru metal nanoparticles upon Se loading, this method produces catalyst that is comparable with the catalyst generated by the colloidal route, generally applicable for metal nanoparticle synthesis. The herein described preparation approach is therefore favorable over the colloidal method due to simplified synthetic protocols, easier scale-up and higher reproducibility.

In the RuSe/C catalysts, a smaller amount of selenium was found to significantly enhance the catalytic activity. However, at high selenium concentrations the catalytic activity was found to be nearly the same as that of samples without selenium modification. Optimum activity is now found at an overall Ru:Se ratio in the vicinity of 94:6. At high selenium concentration the formation of lamellar ruthenium selenide coverage of ruthenium core particles is observed. This structure represents a catalytically inactive crystalline Ru_xSe_y compound, which has a different structure to that of the low selenium loaded, high active catalyst.

Acknowledgements KSN thanks Dr. E.R. Savinova for initiating this work and for useful suggestions. We also thank Dr. D. Alber for the NAA measurements and A. Havemann for assistance in the laboratory. Financial support from the Federal Ministry of Education and Research (BMBF) in the frame of the network "O_2-RedNet" (contract number 03 SF 0302) is gratefully acknowledged. Useful suggestions from the referees are highly appreciated.

References

1. Adzic RR (1998) In: Lipowski J, Ross PN (eds) Electrocatalysis. Wiley-VCH, New York
2. Toda T, Igarashi H, Uchida H, Watanabe M (1999) J Electrochem Soc 146:3750
3. Paulus UA, Schmidt TJ, Gasteiger HA, Behm RJ (2001) J Electrochem Soc 495:134

4. Yang H, Vogel W, Lamy C, Alonso-Vante N (2004) J Phys Chem B 108:11024
5. Maillard F, Martin M, Gloaguen F, Leger JM (2002) Electrochim Acta 47:3431
6. Li W, Zhou W, Li H, Zhou Z, Zhou B, Sun G, Xin Q (2004) Electrochim Acta 49:1045
7. Alonso-Vante N, Borthern P, Fieber-Erdmann M, Strehblow HH, Holub-Krappe E (2000) Electrochim Acta 45:4227
8. Dassenoy F, Vogel W, Alonso-Vante N (2002) J Phys Chem B 106:12152
9. Le Rhun V, Alonso-Vante N (2000) J New Mater Electrochem Syst 3:331
10. Bron M, Bogdanoff P, Fiechter S, Hilgendorff M, Radnik J, Dorbandt I, Schulenburg H, Tributsch H (2001) J Electroanal Chem 517:85
11. Tributsch H, Bron M, Hilgendorff M, Schulenburg H, Dorbandt I, Eyert V, Bogdanoff P, Fiechter S (2001) J Appl Electrochem 31:739
12. Zaikovskii VI, Nagabhushana KS, Kriventsov VV, Loponov KN, Cherepanova SV, Kvon RI, Bönnemann H, Kochubey DI, Savinova ER (2006) J Phys Chem B 110:6881
13. Gonzaler-Huerta RG, Chavez-Carvayar JA, Solorza-Feria O (2006) J Power Sources 153:11
14. Hilgendorff M, Diesner K, Schulenburg H, Bogdanoff P, Bron M, Fiechter S (2002) J New Mater Electrochem Syst 5:71
15. Colmenares L, Jusys Z, Behm RJ (2006) Langmuir 22:10437
16. Bönnemann H, Endruschat U, Hormes J, Köhl S, Kruse S, Modrow H, Mörtel R, Nagabhushana KS (2004) Fuel Cells 4:297
17. Ishiguro A, Nakajima T, Iwata T, Fujita M, Minato T, Kiyotaki F, Izumi Y, Aika K-I, Uchida M, Kimoto K, Matsui Y, Wakatsuki Y (2002) Chem Eur J 8:3260
18. Hadzi-Jordanov S, Angerstein-Kozlowska H, Vuković M, Conway BE (1977) J Phys Chem 81:2271
19. Zehl G, Dorbandt I, Fiechter S, Bogdanoff P (2007) J New Mat Electrochem Syst (submitted)
20. Loponov KN, Kriventsov VV, Kochubey DI, Nagabhushana KS, Boennemann H, Savinova ER (submitted) J Phys Chem B
21. Bron M, Bogdanoff P, Fiechter S, Dorbandt I, Hilgendorff M, Schulenburg H, Tributsch H (2001) J Electroanalyt Chem 500:510